Uniwersytet Gdański

HotHybrids – project summary

dr inż. Anna Pancielejko
mgr inż. Hanna Zagórska

www.ug.edu.pl

17/10/2024

Pioneering hybrid materials for CO_2 photoconversion

Acronym: HotHybrids

Financing institution: National Centre for Research and Development and Norwegian Funds

Funding amount: PLN 863,750.00

Project duration: 01.04.2022 – 30.04.2024

https://hothybrids.ug.edu.pl/

https://www.youtube.com/watch?v=vyrQsLgIm90&ab_channel=KatedraTechnologii%C5%9ArodowiskaWChUG

Norway grants

Rzeczpospolita Polska

NCBR National Centre for Research and Development

„Pioneering hybrid materials for CO_2 photoconversion", no NOR/SGS/HotHybrids/0130/2020-00. Project financed by the Financial Mechanism of the European Economic Area (EEA) and the Norwegian Financial Mechanism 2014-2021.

Project staff

People employed in the project:

Head of the project: prof. dr hab. inż. Adriana Zaleska-Medynska

Executor: dr inż. Anna Pancielejko

Executor: mgr inż. Hanna Zagórska

People supporting the project:

dr Magdalena Miodyńska-Melzer

dr inż. Anna Gołąbiewska

dr inż. Emilia Gontarek-Castro

mgr Mateusz Baluk

„Pioneering hybrid materials for CO_2 photoconversion", no NOR/SGS/HotHybrids/0130/2020-00. Project financed by the Financial Mechanism of the European Economic Area (EEA) and the Norwegian Financial Mechanism 2014-2021.

Project goals

The main goal of the HotHybrids project was to develop a class of hybrid materials consisting of new double perovskite nanocrystals (DPNs) and metal-organic frameworks (MOFs) with high activity and selectivity in the photoconversion of CO_2 to valuable hydrocarbons.

<u>The detailed tasks concerned:</u>

- correlation of synthesis methods with morphology, stability, and activity of DPNs;
- finding a method for effective encapsulation of DNPs in MOF structures;
- correlation of MOF composition (metal cations/organic ligand) and synthesis method of DPNs-MOFs hybrids with their morphology, stability and photoactivity;
- understanding the mechanism of CO_2 photoconversion of DPNs-MOFs hybrids;
- development of a synthesis method (laboratory and pilot scale) for the selected hybrid system.

„Pioneering hybrid materials for CO_2 photoconversion", no NOR/SGS/HotHybrids/0130/2020-00. Project financed by the Financial Mechanism of the European Economic Area (EEA) and the Norwegian Financial Mechanism 2014-2021.

Problems in project implementation

1. Synthesis of double perovskites stable in aqueous solution.
2. Encapsulation of perovskites in a metal-organic framework structure.
3. Obtaining hybrids active in the CO_2 photoconversion reaction in aqueous solution.
4. Obtaining a scaled-up hybrid with proper morphology and high activity in the photocatalytic hydrogen generation reaction.

„Pioneering hybrid materials for CO_2 photoconversion", no NOR/SGS/HotHybrids/0130/2020-00. Project financed by the Financial Mechanism of the European Economic Area (EEA) and the Norwegian Financial Mechanism 2014-2021.

Project indicators

Publications:

- Pancielejko A. et al. Rational designing of TiO_2-X@$Cs_3Bi_2X_9$ nanocomposite for boosted hydrogen evolution, Catalysis Today (2024) 432, 114626.
- Pancielejko A. et al. $CuGaS_2$@NH_2-MIL-125(Ti) nanocomposite: Unveiling a promising catalyst for photocatalytic hydrogen generation, International Journal of Hydrogen Energy (2024) 79, 186-198.
- Głowienke H. et al. Novel room-temperature synthesis of pioneering $CsPbX_3$@(Ce)UiO-66-Y hybrid nanomaterials for boosted photocatalytic hydrogen evolution, Journal of Photochemistry and Photobiology A: Chemistry (2024), 454, 115731.
- Miodyńska M. et al. A comprehensive review of preparation methods, properties, and photocatalytic performance of diverse perovskite structures, Wiadomości Chemiczne (2024), 78, 3-4.
- Pancielejko A. et al. Cu-incorporated NH_2-MIL-125(Ti): A Versatile Visible-Light-Driven Platform for Enhanced Photocatalytic H_2 Generation and CO_2 Photoconversion, Materials Horizons, under review.

Patent application:

- $CuGaS_2$@NH_2-MIL-125(Ti) nanocomposites, method of obtaining them and use of $CuGaS_2$@NH_2-MIL-125(Ti) nanocomposites as a photocatalytic material, P.448194.

„Pioneering hybrid materials for CO_2 photoconversion", no NOR/SGS/HotHybrids/0130/2020-00. Project financed by the Financial Mechanism of the European Economic Area (EEA) and the Norwegian Financial Mechanism 2014-2021.

Catalysis Today 432 (2024) 114626

Contents lists available at ScienceDirect

Catalysis Today

journal homepage: www.elsevier.com/locate/cattod

Rational designing of TiO_2-X@$Cs_3Bi_2X_9$ nanocomposite for boosted hydrogen evolution

Anna Pancielejko[a,*], Magdalena Miodyńska[a], Hanna Głowienke[a], Anna Gołąbiewska[a], Emilia Gontarek-Castro[a], Tomasz Klimczuk[b], Mirosław Krawczyk[c], Grzegorz Trykowski[d], Adriana Zaleska-Medynska[a,*]

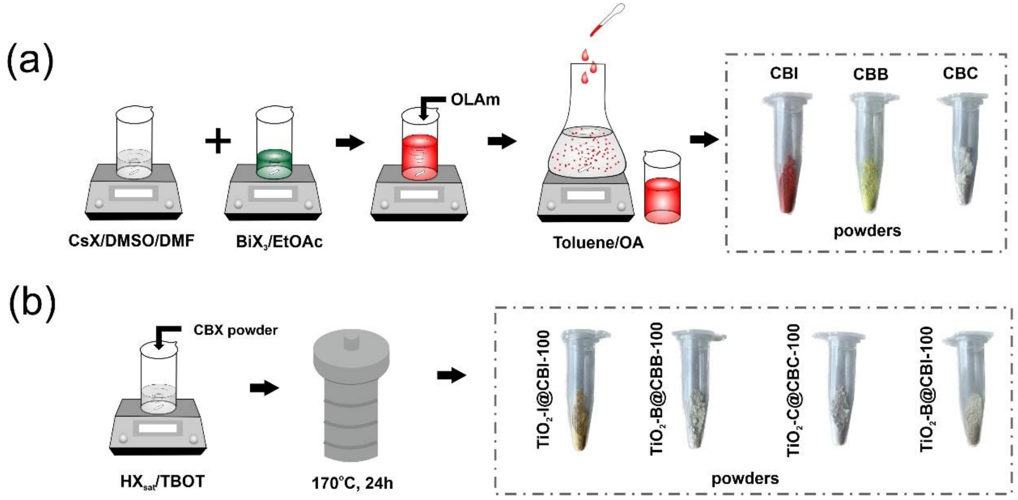

Fig. 1. Schematic diagram of the two-step preparation process of a) $Cs_3Bi_2X_9$ perovskites and b) TiO_2-X@CBX (X = I, Br, Cl) nanocomposites.

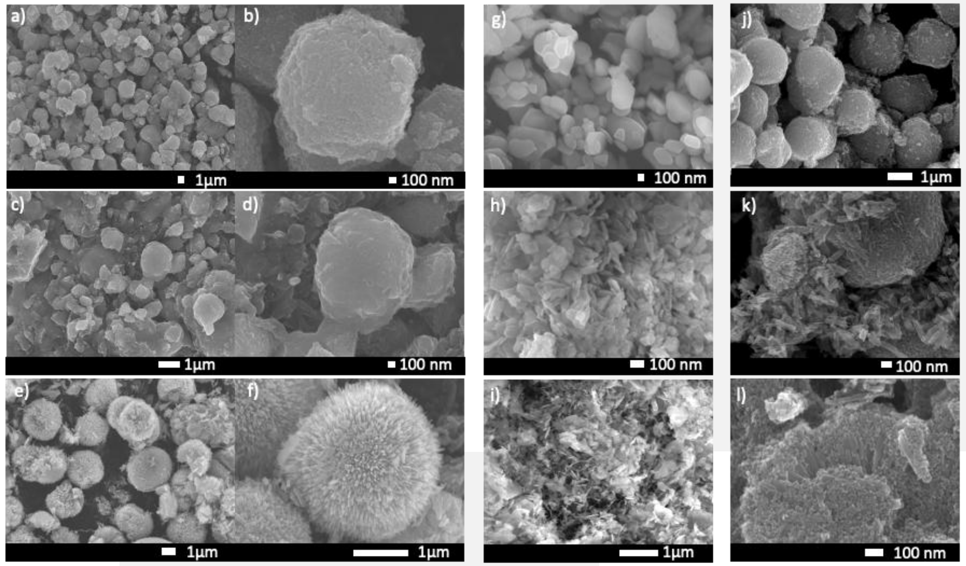

Fig. 2. SEM images of (a-b) TiO_2-I, (c-d) TiO_2-B, (e-f) TiO_2-C, (g) CBI, (h) CBB, (i) CBC, (j) TiO_2-I@CBI-100, (k) TiO_2-Br@CBB-100, (l) TiO_2-C@CBC-100.

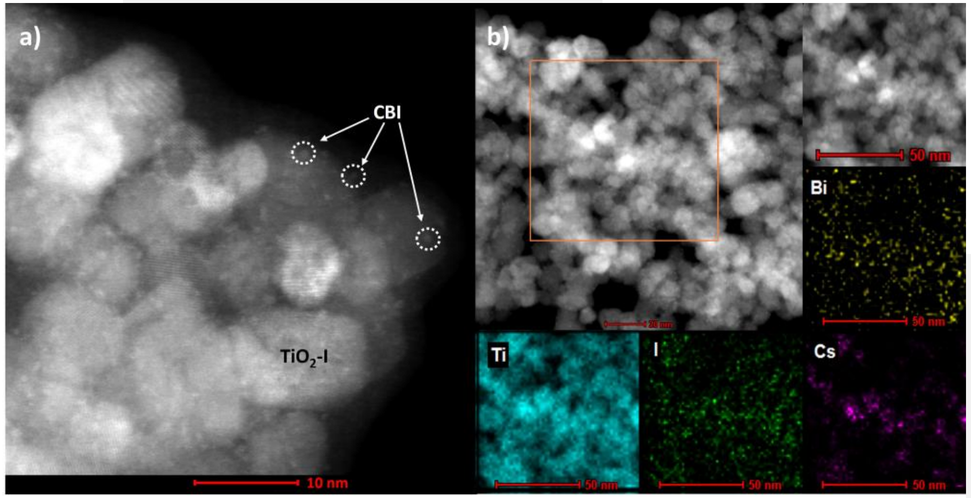

Fig. 3. STEM-EDS analysis of TiO_2-I@CBI-100 with elemental mapping (Bi, Ti, I and Cs).

„Pioneering hybrid materials for CO_2 photoconversion", no NOR/SGS/HotHybrids/0130/2020-00. Project financed by the Financial Mechanism of the European Economic Area (EEA) and the Norwegian Financial Mechanism 2014-2021.

Catalysis Today 432 (2024) 114626

Contents lists available at ScienceDirect

Catalysis Today

journal homepage: www.elsevier.com/locate/cattod

Rational designing of TiO_2-X@$Cs_3Bi_2X_9$ nanocomposite for boosted hydrogen evolution

Anna Pancielejko [a,*], Magdalena Miodyńska [a], Hanna Głowienke [a], Anna Gołąbiewska [a], Emilia Gontarek-Castro [a], Tomasz Klimczuk [b], Mirosław Krawczyk [c], Grzegorz Trykowski [d], Adriana Zaleska-Medynska [a,*]

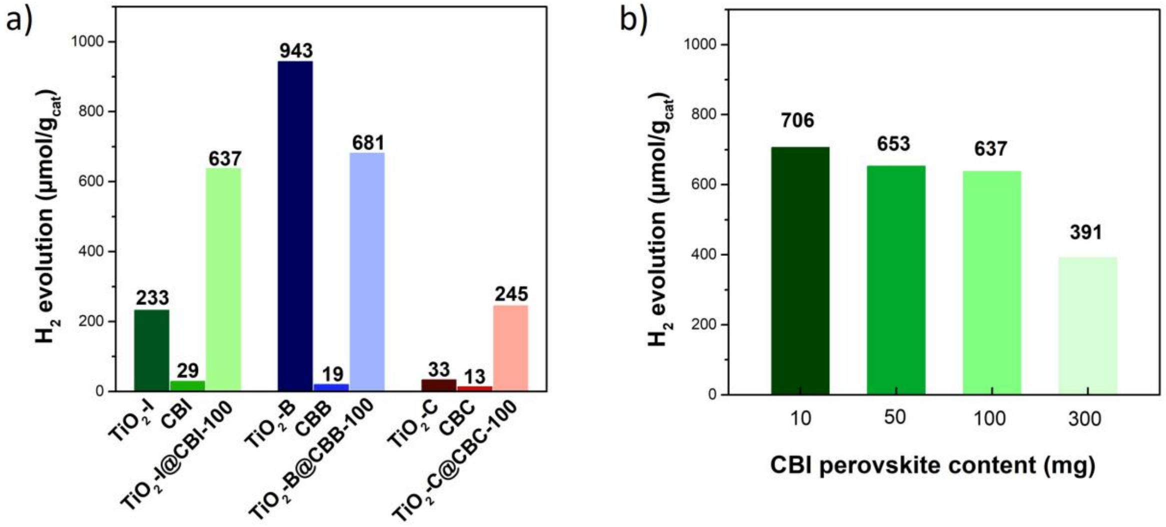

Fig. 4. Photocatalytic H_2 generation of a) TiO_2-X, CBX, and TiO_2-X@CBX-100 nanocomposites, and b) TiO_2-I@CBI nanocomposites differ in CBI amount after 240 minutes of UV-Vis irradiation.

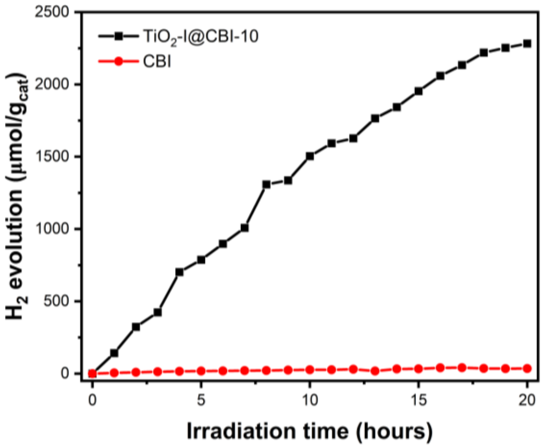

Fig. 5. Long-term stability of TiO_2-I@CBI-10 and CBI materials.

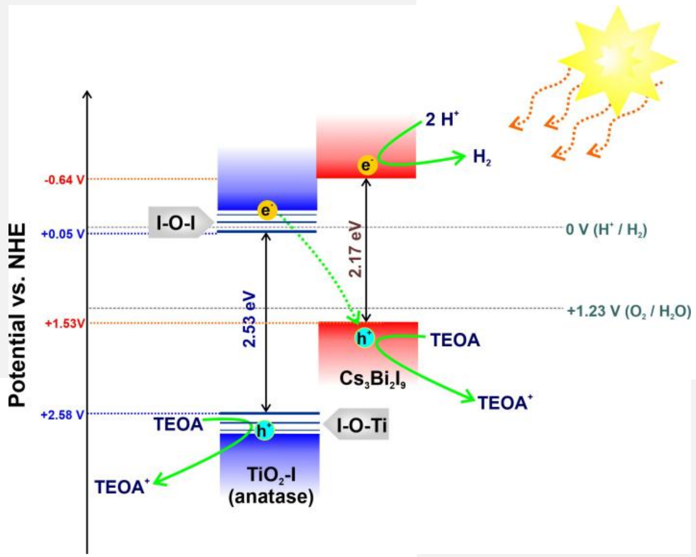

Fig. 6. Schematic separation and charge transfer diagram during photocatalytic hydrogen evolution in the TiO_2-I@CBI-10 photocatalyst.

„Pioneering hybrid materials for CO_2 photoconversion", no NOR/SGS/HotHybrids/0130/2020-00. Project financed by the Financial Mechanism of the European Economic Area (EEA) and the Norwegian Financial Mechanism 2014-2021.

International Journal of Hydrogen Energy 79 (2024) 186–198

Contents lists available at ScienceDirect

International Journal of Hydrogen Energy

journal homepage: www.elsevier.com/locate/he

$CuGaS_2$@NH_2-MIL-125(Ti) nanocomposite: Unveiling a promising catalyst for photocatalytic hydrogen generation

Anna Pancielejko[a,**], Hanna Głowienke[a], Magdalena Miodyńska[a], Anna Gołąbiewska[a], Tomasz Klimczuk[b], Mirosław Krawczyk[c], Krzysztof Matus[d], Adriana Zaleska-Medynska[a,*]

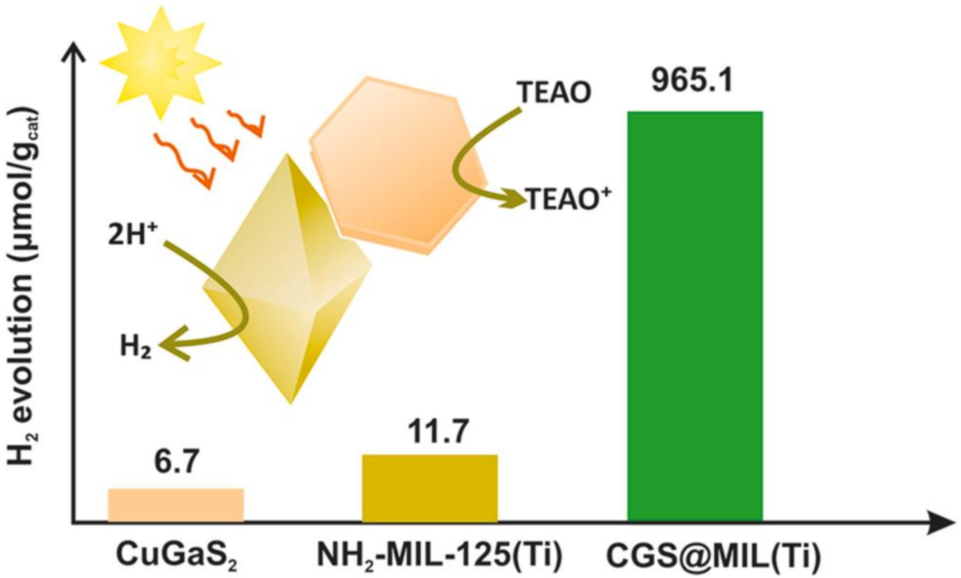

Fig. 7 Schematic diagram illustrating the concepts behind the work on the $CuGaS_2$@NH_2-MIL-125(Ti) material.

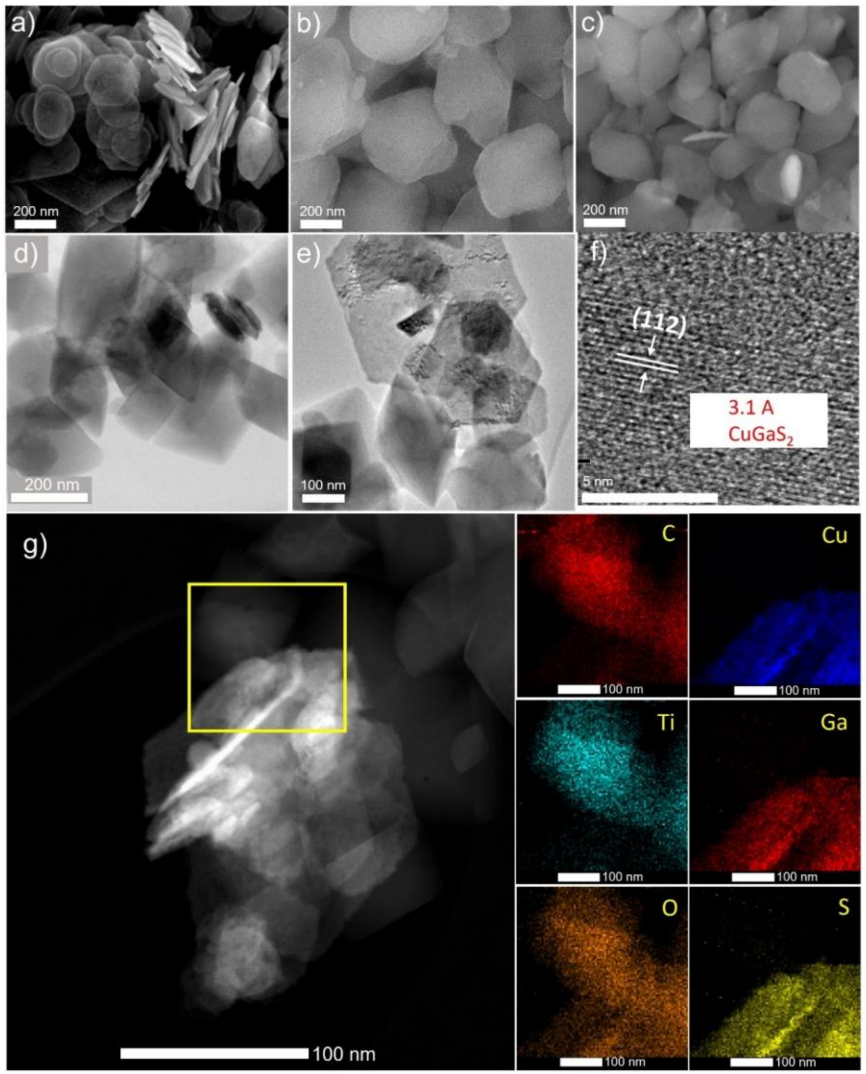

Fig. 8. SEM images of a) $CuGaS_2$, b) NH_2-MIL-125(Ti), c) CGS-30@MIL(Ti), and d) STEM, e) TEM, and f) HRTEM images with elemental mapping of CGS-30@MIL(Ti).

„Pioneering hybrid materials for CO_2 photoconversion”, no NOR/SGS/HotHybrids/0130/2020-00. Project financed by the Financial Mechanism of the European Economic Area (EEA) and the Norwegian Financial Mechanism 2014-2021.


International Journal of Hydrogen Energy 79 (2024) 186–198

Contents lists available at ScienceDirect

International Journal of Hydrogen Energy

journal homepage: www.elsevier.com/locate/he

CuGaS$_2$@NH$_2$-MIL-125(Ti) nanocomposite: Unveiling a promising catalyst for photocatalytic hydrogen generation

Anna Pancielejko [a,**], Hanna Głowienke [a], Magdalena Miodyńska [a], Anna Gołąbiewska [a], Tomasz Klimczuk [b], Mirosław Krawczyk [c], Krzysztof Matus [d], Adriana Zaleska-Medynska [a,*]

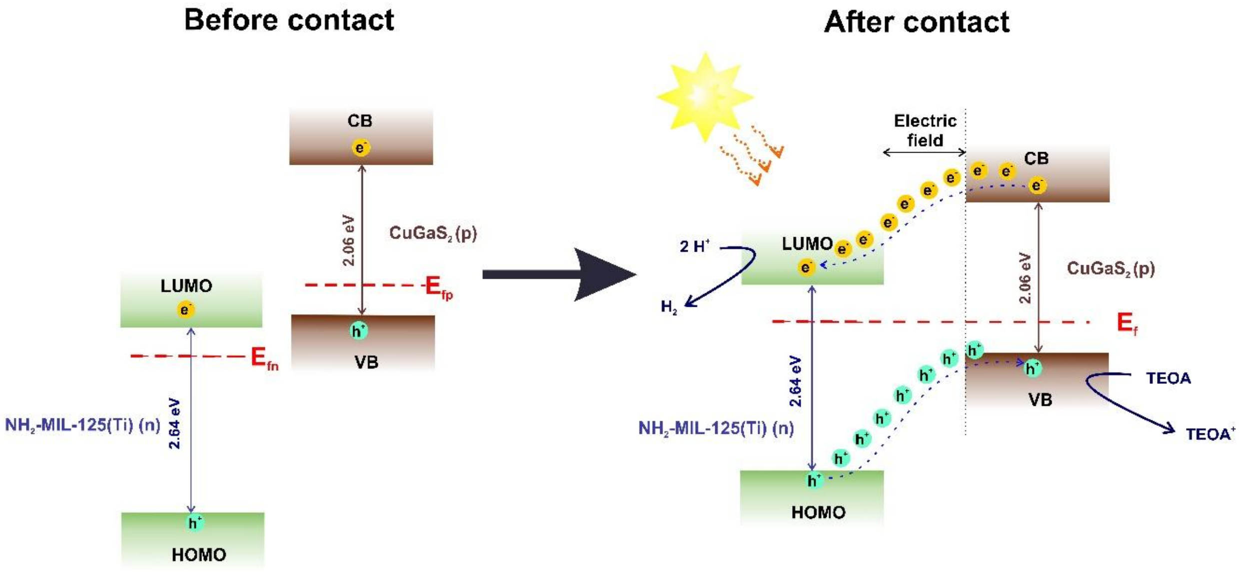

Fig. 10. Schematic diagram of (a) the band energies of NH$_2$-MIL-125(Ti) and CuGaS$_2$ before (a) and after (b) composite formation and the proposed charge transfer and separation process of CuGaS$_2$@NH$_2$-MIL-125(Ti) under UV-Vis radiation.

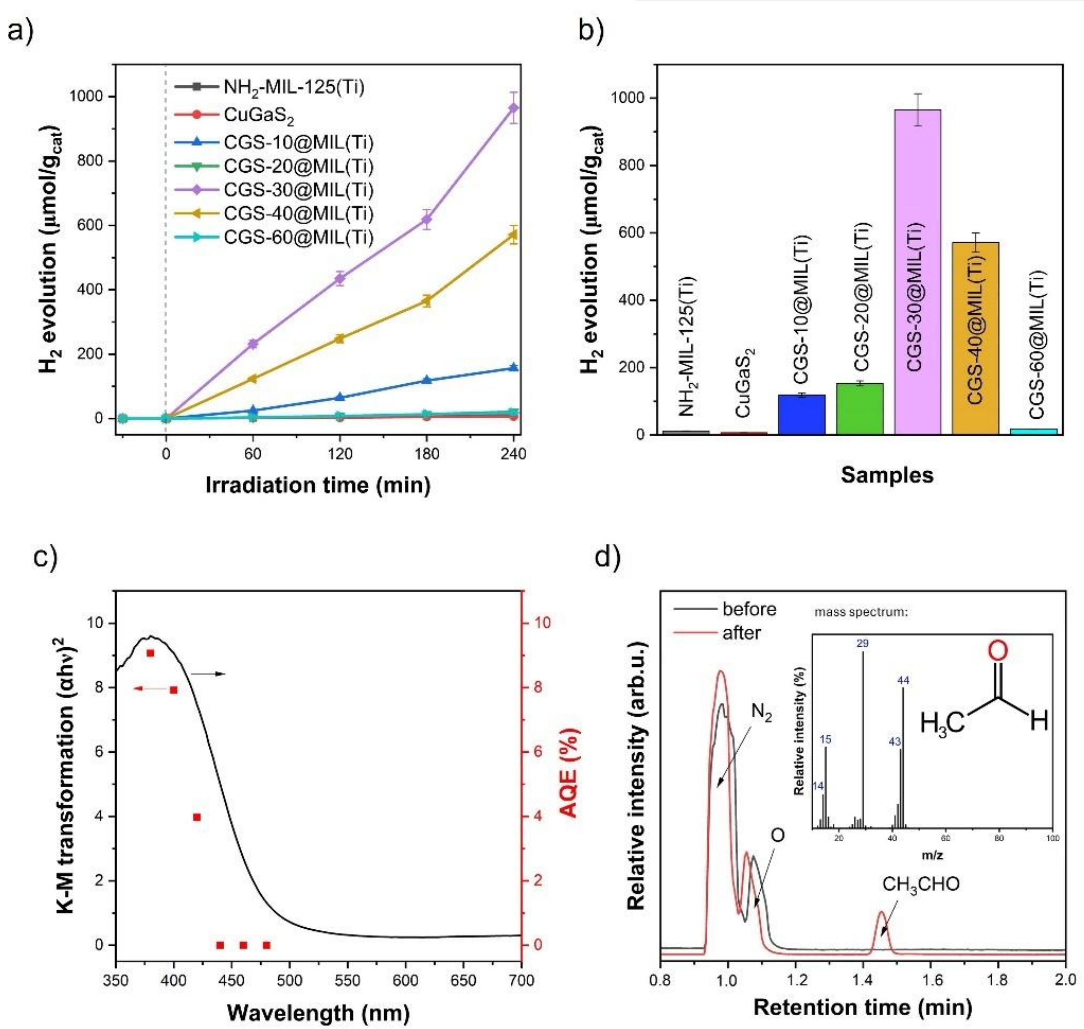

Fig. 9. a). H$_2$ generation rate under the influence of UV-Vis radiation, b) H$_2$ generation efficiency after 4 hours of UV-Vis radiation exposure, c) Action Spectra measurement for the CGS-30@MIL(Ti) sample, and d) GC/MS spectra of the electrolyte before and after the photocatalytic process in the presence of the CGS-30@MIL(Ti) sample.

„Pioneering hybrid materials for CO_2 photoconversion", no NOR/SGS/HotHybrids/0130/2020-00. Project financed by the Financial Mechanism of the European Economic Area (EEA) and the Norwegian Financial Mechanism 2014-2021.

Cu-incorporated NH2-MIL-125(Ti): A Versatile Visible-Light-Driven Platform for Enhanced Photocatalytic H2 Generation and CO2 Photoconversion

Anna Pancielejko [a*], Mateusz A. Baluk [a], Hanna Zagórska [a], Magdalena Miodyńska-Melzer [a], Anna Gołąbiewska [a], Tomasz Klimczuk [b], Mirosław Krawczyk [c], Mirosława Pawlyta [d], Krzysztof Matus [d], Alicja Mikolajczyk [f,g], Henry P. Pinto [h], Aleksandra Pieczyńska [a], Joanna Dołżonek [e], Adriana Zaleska-Medynska [a*]

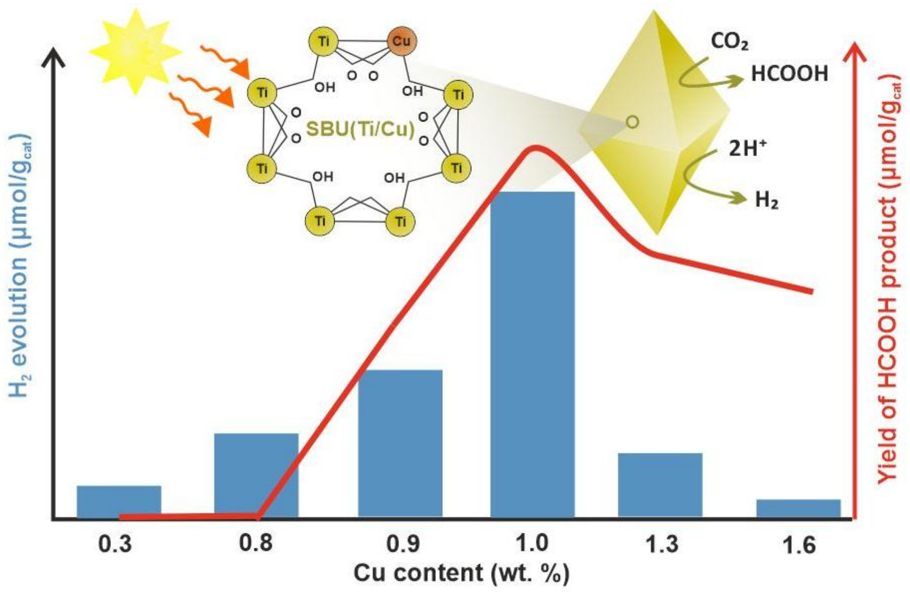

Fig. 11. Schematic diagram illustrating the work concepts for the Cu-NH_2-MIL-125(Ti) series.

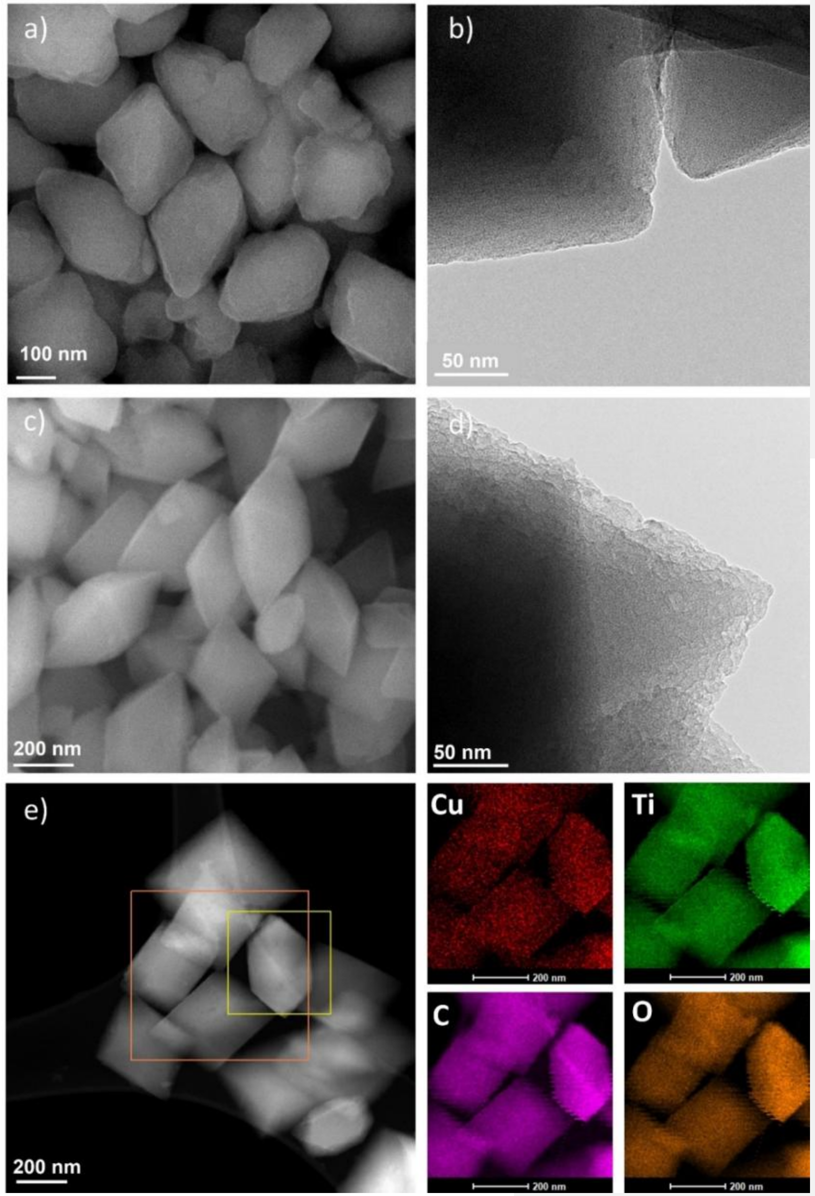

Fig. 12. (a) SEM and (b) TEM images of pristine NH_2- MIL-125(Ti). (c) SEM and (d) TEM images with elemental mapping (Cu, Ti, C, and O) of MIL(Cu/Ti)1.0 sample.

„Pioneering hybrid materials for CO_2 photoconversion", no NOR/SGS/HotHybrids/0130/2020-00. Project financed by the Financial Mechanism of the European Economic Area (EEA) and the Norwegian Financial Mechanism 2014-2021.

Materials Horizons

Cu-incorporated NH2-MIL-125(Ti): A Versatile Visible-Light-Driven Platform for Enhanced Photocatalytic H2 Generation and CO2 Photoconversion

Anna Pancielejko [a], Mateusz A. Baluk [a], Hanna Zagórska [a], Magdalena Miodyńska-Melzer [a], Anna Gołąbiewska [a], Tomasz Klimczuk [b], Mirosław Krawczyk [c], Mirosława Pawlyta [d], Krzysztof Matus [d], Alicja Mikolajczyk [f,g], Henry P. Pinto [h], Aleksandra Pieczyńska [a], Joanna Dołżonek [c], Adriana Zaleska-Medynska [a*]*

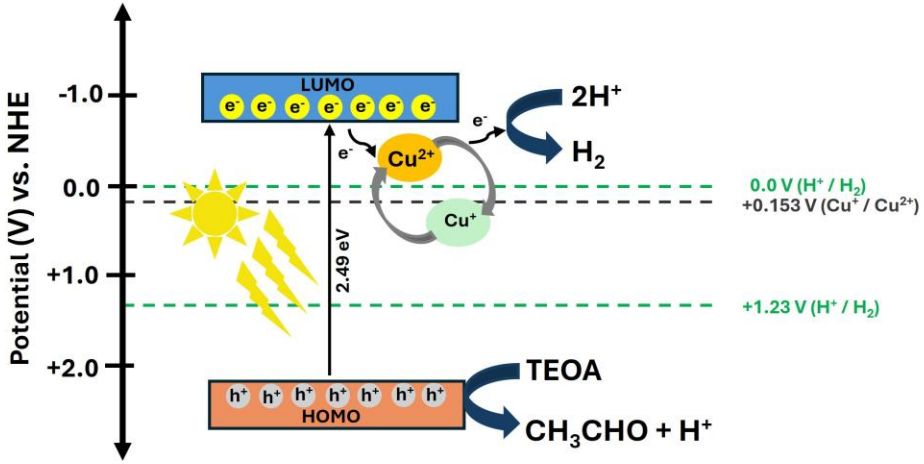

Fig. 14. Proposed mechanism of hydrogen generation in the presence of MIL(Cu/Ti)1.0 photocatalyst.

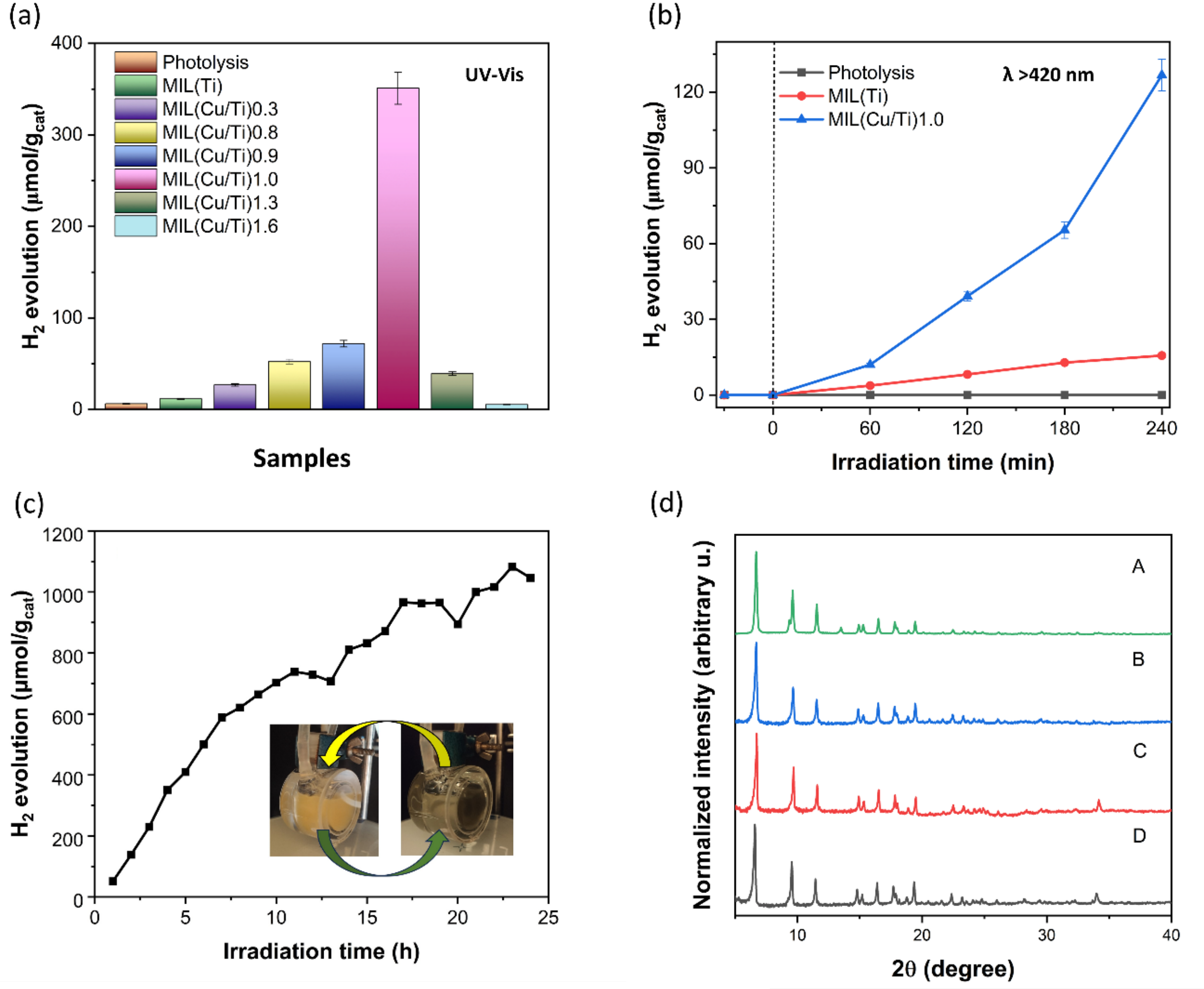

Fig. 13. Photocatalytic hydrogen generation after 4 hours of a) UV-Vis and b) visible irradiation. c) Long-term stability of the most active sample under UV-Vis irradiation. d) XRD diffractograms of MIL(Cu/Ti)1.0 A – before irradiation, B – after 24 hours of UV-Vis radiation, C – after 4 hours of UV-Vis radiation, D - after 4 hours of Vis radiation.

„Pioneering hybrid materials for CO_2 photoconversion", no NOR/SGS/HotHybrids/0130/2020-00. Project financed by the Financial Mechanism of the European Economic Area (EEA) and the Norwegian Financial Mechanism 2014-2021.

Materials Horizons

Cu-incorporated NH2-MIL-125(Ti): A Versatile Visible-Light-Driven Platform for Enhanced Photocatalytic H2 Generation and CO2 Photoconversion

Anna Pancielejko [a], Mateusz A. Baluk [a], Hanna Zagórska [a], Magdalena Miodyńska-Melzer [a], Anna Gołąbiewska [a], Tomasz Klimczuk [b], Mirosław Krawczyk [c], Mirosława Pawlyta [d], Krzysztof Matus [d], Alicja Mikolajczyk [f,g], Henry P. Pinto [h], Aleksandra Pieczyńska [a], Joanna Dołżonek [e], Adriana Zaleska-Medynska [a*]*

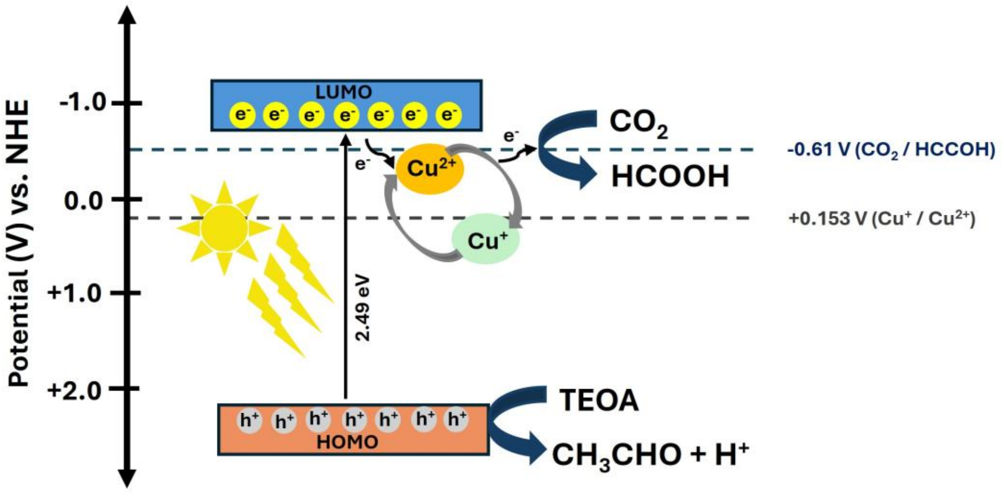

Fig. 17. Proposed mechanism of CO_2 photoconversion in the presence of MIL(Cu/Ti)1.0 photocatalyst.

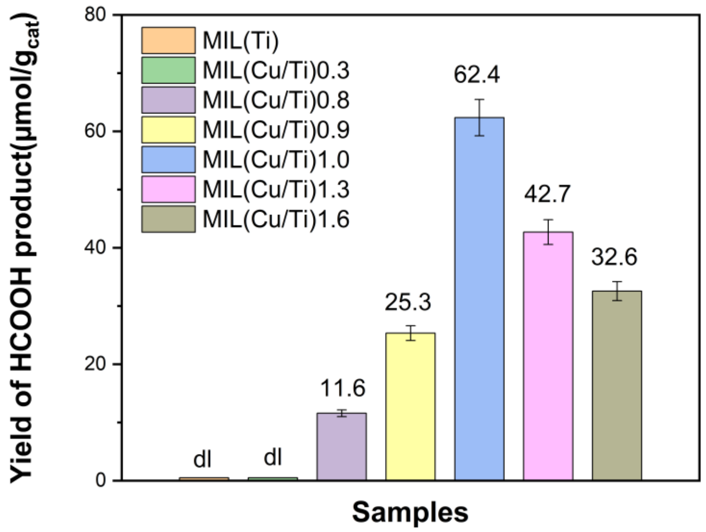

Fig. 15. Efficiency of photoconversion of CO_2 under visible irradiation (dl – detection limit).

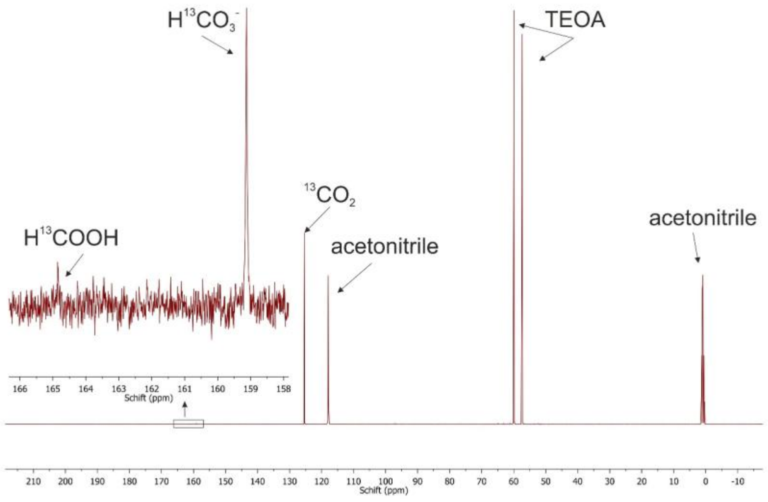

Fig. 16. ^{13}C NMR spectra products detected during photoconversion of $^{13}CO_2$ in the presence of MIL(Cu/Ti)1.0 in visible range

„Pioneering hybrid materials for CO_2 photoconversion", no NOR/SGS/HotHybrids/0130/2020-00. Project financed by the Financial Mechanism of the European Economic Area (EEA) and the Norwegian Financial Mechanism 2014-2021.

Journal of Photochemistry & Photobiology, A: Chemistry 454 (2024) 115731

Contents lists available at ScienceDirect

Journal of Photochemistry & Photobiology, A: Chemistry

journal homepage: www.elsevier.com/locate/jphotochem

Novel room-temperature synthesis of pioneering $CsPbX_3$@(Ce)UiO-66-Y hybrid nanomaterials for boosted photocatalytic hydrogen evolution

Hanna Głowienke [a], Anna Pancielejko [a,*], Magdalena Miodyńska [a], Anna Gołąbiewska [a], Emilia Gontarek-Castro [a], Tomasz Klimczuk [b], Mirosław Krawczyk [c], Mirosława Pawlyta [d], Adriana Zaleska-Medynska [a,*]

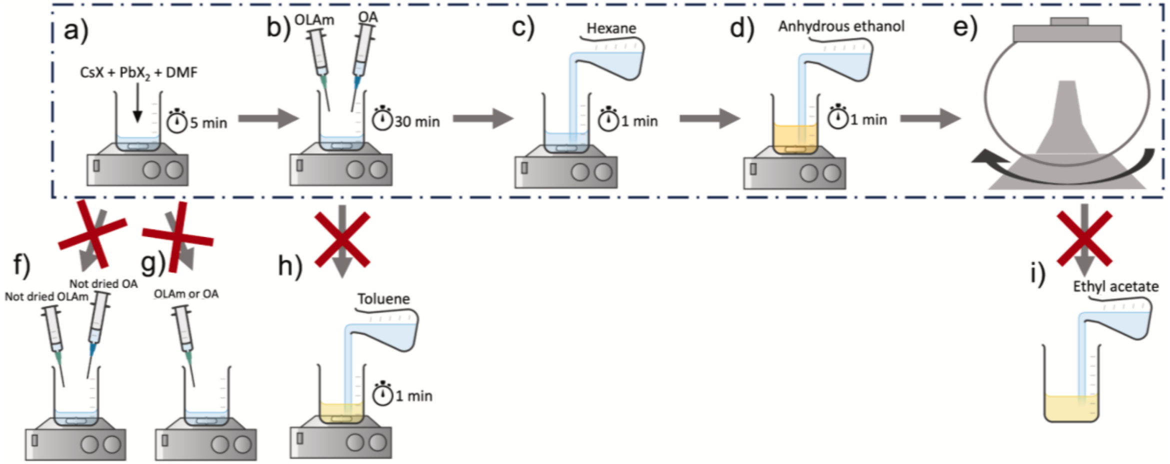

Fig. 18. (a-e) Schematic diagram of the successful synthesis route of $CsPbX_3$ (X = Br, I) perovskites along with (f-i) synthesis routes that did not allow obtaining the desired product.

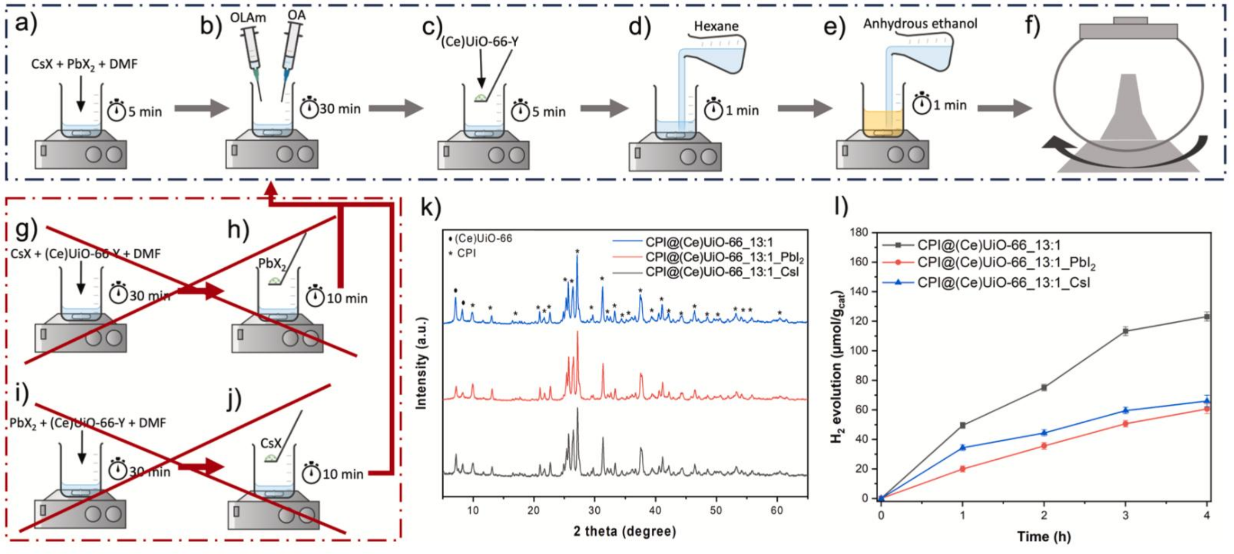

Fig. 19. (a-f) Schematic diagram of the successful synthesis route of $CsPbX_3$@(Ce)UiO-66-Y (X = Br, I; Y = H, Br, NH_2) hybrids along with (g-j) problematic routes, k) XRD patterns for hybrids obtained with different order of reagent addition, l) efficiency of photocatalytic hydrogen evolution of hybrids obtained with different order of reagent addition.

„Pioneering hybrid materials for CO_2 photoconversion", no NOR/SGS/HotHybrids/0130/2020-00. Project financed by the Financial Mechanism of the European Economic Area (EEA) and the Norwegian Financial Mechanism 2014-2021.

Journal of Photochemistry & Photobiology, A: Chemistry 454 (2024) 115731

Contents lists available at ScienceDirect

Journal of Photochemistry & Photobiology, A: Chemistry

journal homepage: www.elsevier.com/locate/jphotochem

Novel room-temperature synthesis of pioneering $CsPbX_3$@(Ce)UiO-66-Y hybrid nanomaterials for boosted photocatalytic hydrogen evolution

Hanna Głowienke [a], Anna Pancielejko [a,*], Magdalena Miodyńska [a], Anna Gołąbiewska [a], Emilia Gontarek-Castro [a], Tomasz Klimczuk [b], Mirosław Krawczyk [c], Mirosława Pawlyta [d], Adriana Zaleska-Medynska [a,*]

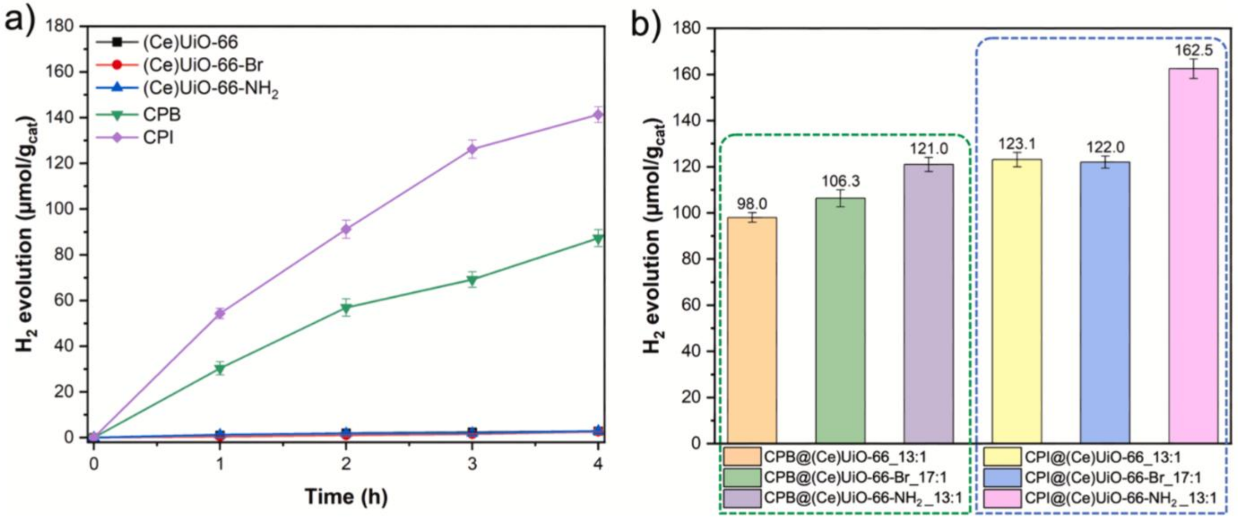

Fig. 20. a) Photocatalytic hydrogen generation efficiency of perovskites and MOFs and b) photocatalytic hydrogen generation after 4-h reaction using hybrids under UV-Vis radiation.

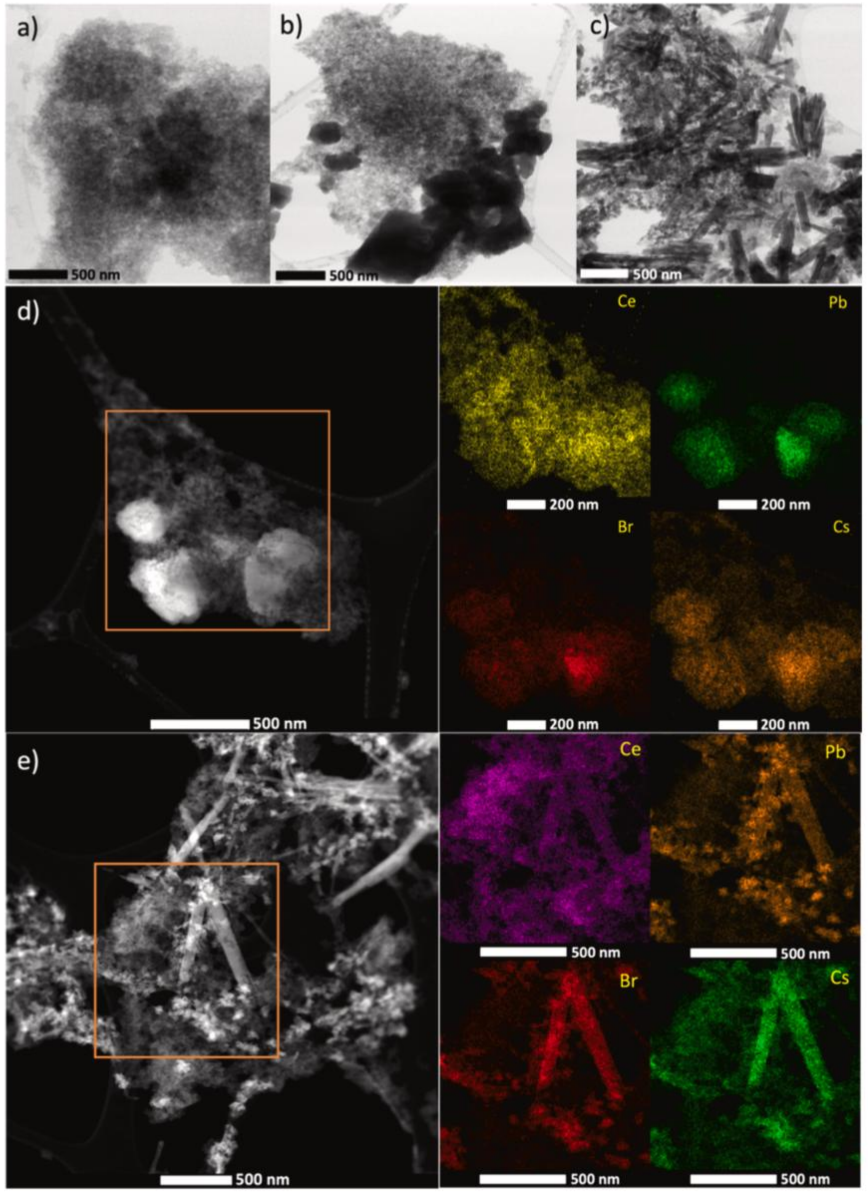

Fig. 21. TEM images a) (Ce)UiO-66-NH_2, b) CPB@(Ce)UiO-66-NH_2_13:1, b) CPI@(Ce)UiO-66-NH_2_13:1 and elemental mapping d) CPB@(Ce)UiO-66-NH_2_13:1 and e) CPI@(Ce)UiO-66-NH_2_13:1.

„Pioneering hybrid materials for CO_2 photoconversion", no NOR/SGS/HotHybrids/0130/2020-00. Project financed by the Financial Mechanism of the European Economic Area (EEA) and the Norwegian Financial Mechanism 2014-2021.

Scale-up of the $SrTiO_3$/MIL-125-NH_2 hybrid production process

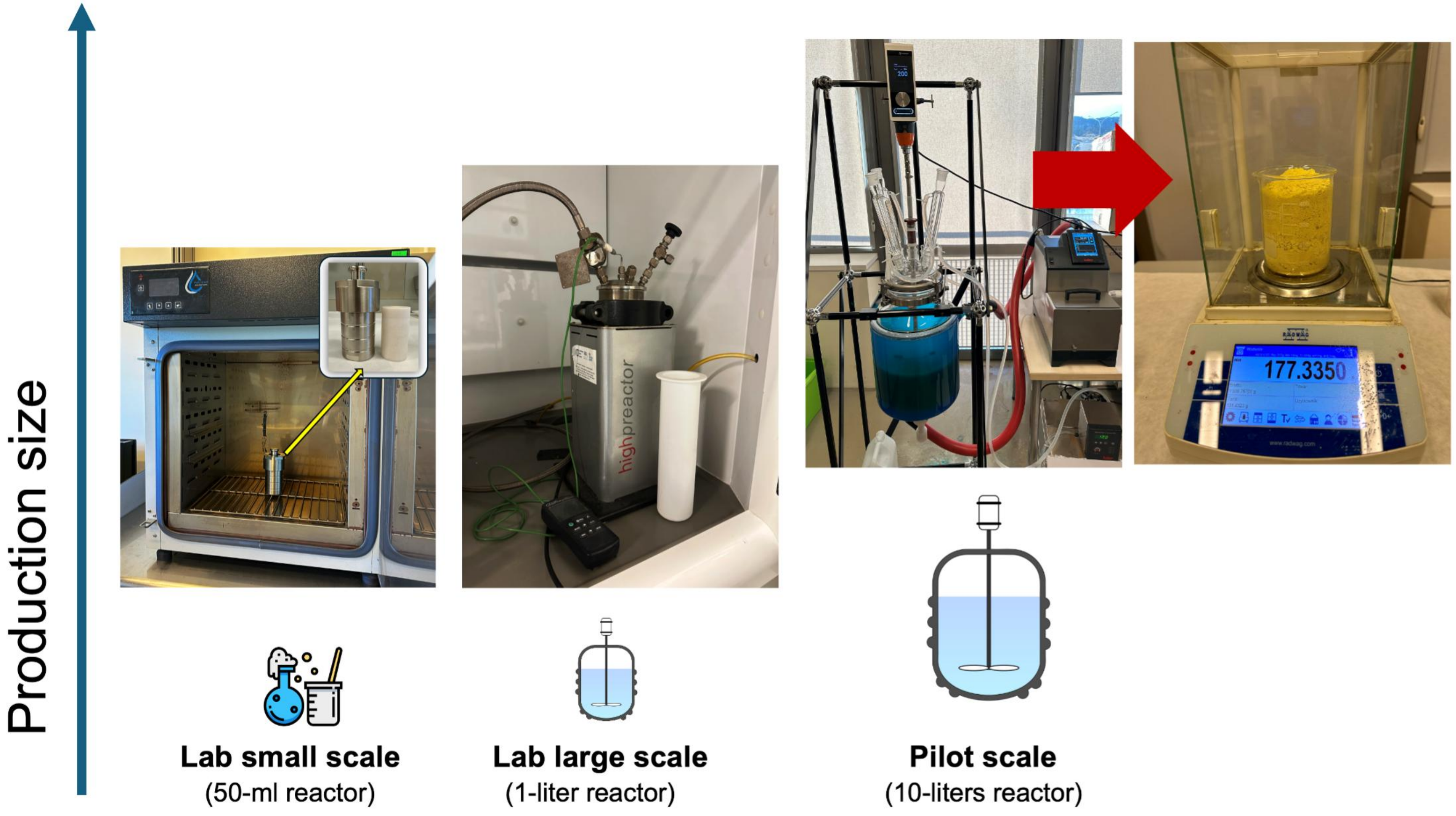

Fig. 22. Diagram showing the subsequent stages of the hybrid synthesis scale-up process.

„Pioneering hybrid materials for CO_2 photoconversion", no NOR/SGS/HotHybrids/0130/2020-00. Project financed by the Financial Mechanism of the European Economic Area (EEA) and the Norwegian Financial Mechanism 2014-2021.

Scale-up of the $SrTiO_3$/MIL-125-NH_2 hybrid production process

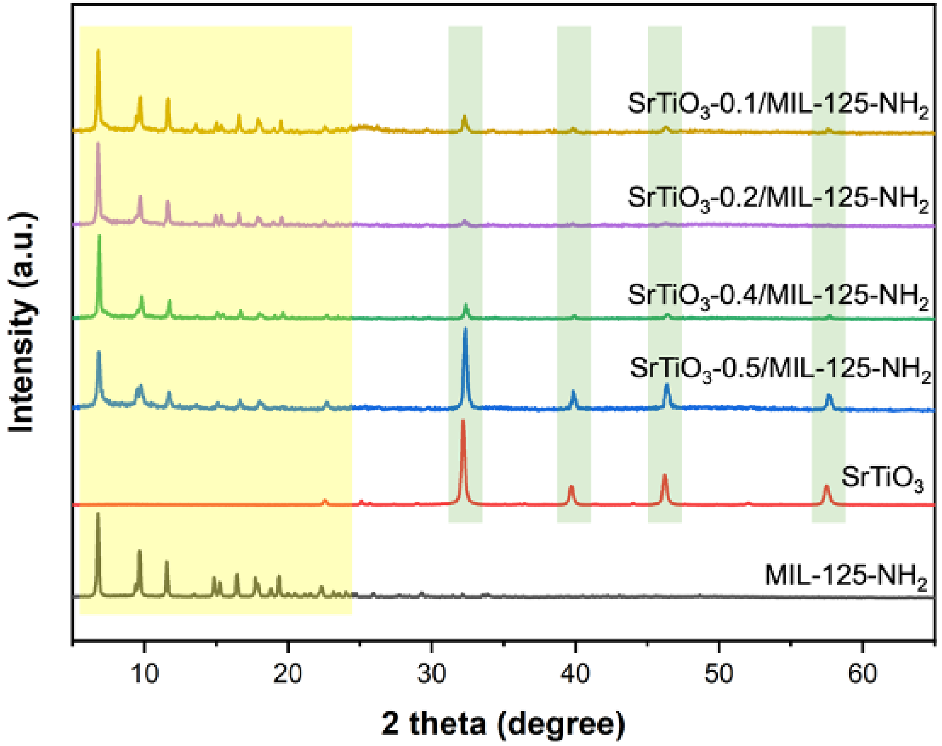

Fig. 23. XRD patterns of pristine NH_2-MIL-125(Ti), $SrTiO_3$ and hybrids obtained on laboratory scale.

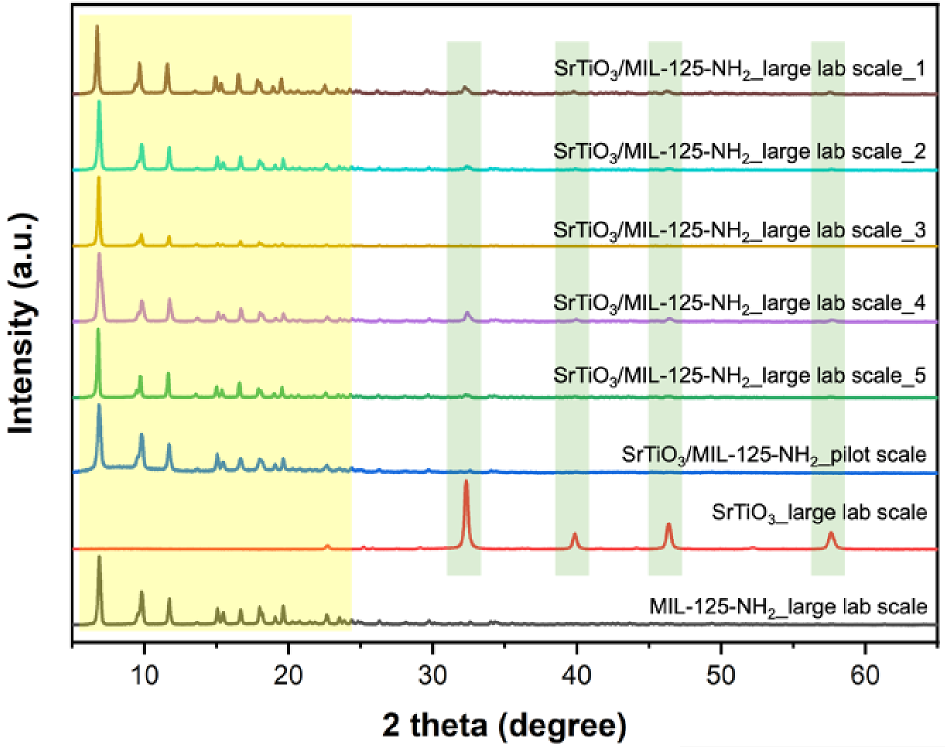

Fig. 24. XRD diffractograms of pristine NH_2-MIL-125(Ti), $SrTiO_3$ and hybrids obtained on large laboratory scale and pilot scale.

„Pioneering hybrid materials for CO_2 photoconversion", no NOR/SGS/HotHybrids/0130/2020-00. Project financed by the Financial Mechanism of the European Economic Area (EEA) and the Norwegian Financial Mechanism 2014-2021.

Scale-up of the $SrTiO_3$/MIL-125-NH_2 hybrid production process

Table 1. Results of the photocatalytic hydrogen generation reaction for samples obtained on a small laboratory scale after each hour of reaction.

Sample label	Amount of H_2 production ($\mu mol/g_{cat}$)				H_2 production rate ($\mu mol/h \cdot g_{cat}$)
	1 h	2 h	3 h	4 h	
MIL-125-NH_2	2.80	5.85	8.63	11.68	2.92
$SrTiO_3$	5.22	10.40	20.55	23.89	5.97
$SrTiO_3$-0.1/MIL-125-NH_2	118.78	161.10	201.83	217.20	54.30
$SrTiO_3$-0.2/MIL-125-NH_2	32.11	60.91	113.81	160.67	40.17
$SrTiO_3$-0.4/MIL-125-NH_2	1.89	3.79	6.30	6.65	1.66
$SrTiO_3$-0.5/MIL-125-NH_2	2.02	4.63	7.14	9.71	2.43

Table 2. Photocatalytic hydrogen generation reaction results for large-scale laboratory and pilot-scale samples after each hour of reaction.

Sample label	Amount of H_2 production ($\mu mol/g_{cat}$)				H_2 production rate ($\mu mol/h \cdot g_{cat}$)
	1h	2h	3h	4h	
$SrTiO_3$/MIL-125-NH_2_large lab scale_1	3.30	7.90	14.34	19.14	4.79
$SrTiO_3$/MIL-125-NH_2_large lab scale_2	10.10	19.94	32.59	44.82	11.21
$SrTiO_3$/MIL-125-NH_2_large lab scale_3	3.35	9.22	17.47	26.34	6.59
$SrTiO_3$/MIL-125-NH_2_large lab scale_4	5.01	11.83	18.91	23.77	5.94
$SrTiO_3$/MIL-125-NH_2_large lab scale_5	2.23	5.98	8.42	10.25	2.56
$SrTiO_3$/MIL-125-NH_2_pilot scale	0.27	0.46	0.82	1.07	0.27
$SrTiO_3$_large lab scale	139.16	239.16	307.43	354.30	88.58
MIL-125-NH_2_large lab scale	22.46	48.08	65.73	82.36	20.59

„Pioneering hybrid materials for CO_2 photoconversion", no NOR/SGS/HotHybrids/0130/2020-00. Project financed by the Financial Mechanism of the European Economic Area (EEA) and the Norwegian Financial Mechanism 2014-2021.

Scale-up of the $SrTiO_3$/MIL-125-NH_2 hybrid production process

Flow chart

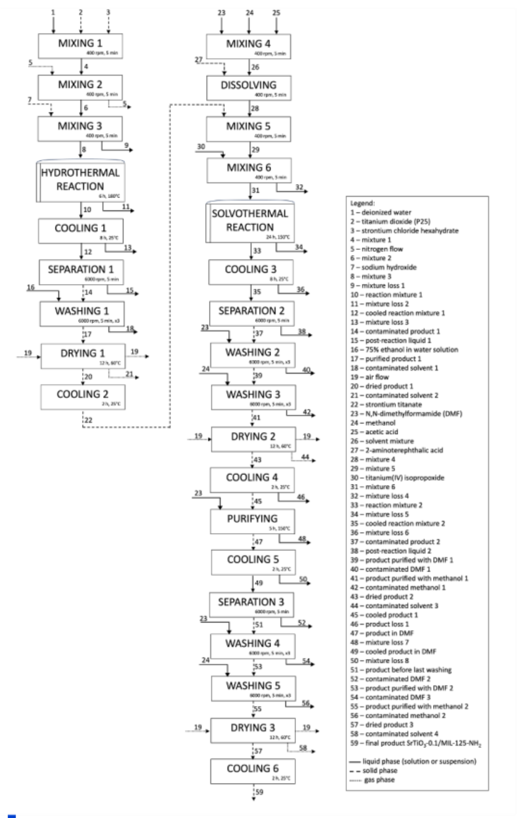

Mass balance

No.	Process unit	INPUT Stream	Mass (g)	Calculations	OUTPUT Stream	Mass (g)	Calculations
1	Mixing 1	Deionized water	49.940	-	Mixture 1	52.112	m_1 = 49.940 g + 0.502 g + 1.670 g = 52.112 g
		Titanium dioxide	0.502	-			
		Strontium chloride hexahydrate	1.670	-			
		SUM	**52.112**		**SUM**	**52.112**	
2	Mixing 2	Mixture 1	52.112	-	Mixture 2	52.112	-
		SUM	**52.112**		**SUM**	**52.112**	
3	Mixing 3	Mixture 2	52.112	-	Mixture 3	52.937	-
		Sodium hydroxide	2.031	-	Mixture loss 1	1.206	$m_{Mixture\ loss\ 1}$ = 54.143 g – 52.937 g = 1.206 g
		SUM	**54.143**		**SUM**	**54.143**	
4	Hydrothermal reaction	Mixture 3	52.937	-	Reaction mixture 1	52.845	-
					Mixture loss 2	0.092	$m_{Mixture\ loss\ 2}$ = 52.937 g – 52.845 g = 0.092 g
		SUM	**52.937**		**SUM**	**52.937**	
5	Cooling 1	Reaction mixture 1	52.845	-	Cooled reaction mixture 1	52.600	-
					Mixture loss 3	0.245	$m_{Mixture\ loss\ 3}$ = 52.845 g – 52.600 g = 0.245 g
		SUM	**52.845**		**SUM**	**52.845**	
6	Separation 1	Cooled reaction mixture 1	52.600	-	Contaminated product 1	2.608	-
					Post-reaction liquid 1	49.992	$m_{Post\text{-}reaction\ liquid\ 1}$ = 52.600 g – 2.608 g = 49.992 g
		SUM	**52.600**		**SUM**	**52.600**	
7	Washing 1	Contaminated product 1	2.608	-	Purified product 1	2.378	After 1st washing: 2.529 g After 2nd washing: 2.414 g After 3rd washing: 2.378 g
		75% ethanol in water	100.719	1st washing: 33.621 g 2nd washing: 33.509 g 3rd washing: 33.589 g Summary: 100.719 g	Contaminated solvent 1	100.949	$m_{Contaminated\ solvent\ 1}$ = 100.719 g + (2.608 g – 2.378 g) = 100.949 g
		SUM	**103.327**		**SUM**	**103.327**	
8	Drying 1	Purified product 1	2.378	-	Dried product 1	1.168	-
					Contaminated solvent 2	1.210	$m_{Contaminated\ solvent\ 2}$ = 2.378 g – 1.168 g = 1.210 g
		SUM	**2.378**		**SUM**	**2.378**	
9	Cooling 2	Dried product 1	1.168	-	Strontium titanate	1.168	-
		SUM	**1.168**		**SUM**	**1.168**	
10	Mixing 4	N,N-dimethylformamide	16.941	-	Solvent mixture	20.536	$m_{Solvent\ mixture}$ = 16.941 g + 1.582 g + 2.013 g = 20.536 g
		Methanol	1.582	-			
		Acetic acid	2.013	-			
		SUM	**20.536**		**SUM**	**20.536**	
11	Dissolving	Solvent mixture	20.536	-	Mixture 4	21.079	$m_{Mixture\ 4}$ = 20.536 g + 0.543 g = 21.079 g
		2-aminoterephthalic acid	0.543	-			
		SUM	**21.079**		**SUM**	**21.079**	
12	Mixing 5	Mixture 4	21.079	-	Mixture 5	21.104	$m_{Mixture\ 4}$ = 21.079 g + 0.025 g = 21.104 g
		Strontium titanate	0.025	-			
		SUM	**21.104**		**SUM**	**21.104**	
13	Mixing 6	Mixture 5	21.104	-	Mixture 6	21.005	-
		Titanium(IV) isopropoxide	0.553	-	Mixture loss 4	0.099	$m_{Mixture\ loss\ 4}$ = 21.104 g – 21.005 g = 0.099 g
		SUM	**21.657**		**SUM**	**21.657**	
14	Solvothermal reaction	Mixture 6	21.005	-	Reaction mixture 2	20.735	-
					Mixture loss 5	0.270	$m_{Mixture\ loss\ 5}$ = 21.005 g – 20.735 g = 0.270 g
		SUM	**21.005**		**SUM**	**21.005**	
15	Cooling 3	Reaction mixture 2	20.735	-	Cooled reaction mixture 2	20.439	-
					Mixture loss 6	0.296	$m_{Mixture\ loss\ 6}$ = 20.735 g – 20.439 g = 0.296 g
		SUM	**20.735**		**SUM**	**20.735**	
16	Separation 2	Cooled reaction mixture 2	20.439	-	Contaminated product 2	1.923	-
					Post-reaction liquid 2	18.516	$m_{Post\text{-}reaction\ liquid\ 2}$ = 20.439 g – 1.923 g = 18.516 g
		SUM	**20.439**		**SUM**	**20.439**	
17	Washing 2	Contaminated product 2	1.923	-	Product purified with DMF 1	1.698	After 1st washing: 1.703 g After 2nd washing: 1.699 g After 3rd washing: 1.698 g
		N,N-dimethylformamide	81.748	1st washing: 27.329 g 2nd washing: 27.154 g 3rd washing: 27.265 g Summary: 81.748 g	Contaminated DMF 1	81.973	$m_{Contaminated\ DMF\ 1}$ = 81.748 g + (1.923 g - 1.698 g) = 81.973 g
		SUM	**83.671**		**SUM**	**83.671**	
18	Washing 3	Product purified with DMF 1	1.698	-	Product purified with methanol 1	1.342	After 1st washing: 1.497 g After 2nd washing: 1.401 g After 3rd washing: 1.342 g
		Methanol	67.995	1st washing: 22.597 g 2nd washing: 22.766 g 3rd washing: 22.632 g Summary: 67.995 g	Contaminated methanol 1	68.351	$m_{Contaminated\ methanol\ 1}$ = 67.995 g + (1.698 g – 1.342 g) = 68.351 g
		SUM	**69.693**		**SUM**	**69.693**	
19	Drying 2	Product purified with methanol 1	1.342	-	Dried product 2	0.318	-
					Contaminated solvent 3	1.024	$m_{Contaminated\ solvent\ 3}$ = 1.342 g – 0.318 g = 1.024 g
		SUM	**1.342**		**SUM**	**1.342**	
20	Cooling 4	Dried product 2	0.318	-	Cooled product 1	0.317	-
					Product loss 1	0.001	$m_{Product\ loss\ 1}$ = 0.318 g – 0.317 g = 0.001 g
		SUM	**0.318**		**SUM**	**0.318**	
21	Purifying	Cooled product 1	0.317	-	Product in DMF	36.593	-
		N,N-dimethylformamide	36.613	-	Mixture loss 7	0.337	$m_{Mixture\ loss\ 7}$ = 36.613 g + 0.317 g – 36.593 g = 0.337 g
		SUM	**36.930**		**SUM**	**36.930**	
22	Cooling 5	Product in DMF	36.593	-	Cooled product in DMF	36.484	-
					Mixture loss 8	0.109	$m_{Mixture\ loss\ 8}$ = 36.593 g – 36.484 g = 0.109 g
		SUM	**36.593**		**SUM**	**36.593**	
23	Separation 3	Cooled product in DMF	36.484	-	Product before last washing	1.618	-
					Contaminated DMF 2	34.866	$m_{Contaminated\ DMF\ 2}$ = 36.484 g – 1.618 g = 34.866 g
		SUM	**36.484**		**SUM**	**36.484**	
24	Washing 4	Product before last washing	1.618	-	Product purified with DMF 2	1.480	After 1st washing: 1.488 g After 2nd washing: [illegible] After 3rd washing: 1.480 g
		N,N-dimethylformamide	81.773	1st washing: 27.244 g 2nd washing: 27.361 g 3rd washing: 27.168 g Summary: 81.773 g	Contaminated DMF 3	81.911	$m_{Contaminated\ DMF\ 3}$ = 81.773 g + (1.618 g - 1.480 g) = 81.911 g
		SUM	**83.391**		**SUM**	**83.391**	
25	Washing 5	Product purified with DMF 2	1.480	-	Product purified with methanol 2	1.209	After 1st washing: 1.374 g After 2nd washing: 1.289 g After 3rd washing: 1.209 g
		Methanol	67.879	1st washing: 22.584 g 2nd washing: 22.700 g 3rd washing: 22.595 g Summary: 67.879 g	Contaminated methanol 2	68.150	$m_{Contaminated\ methanol\ 2}$ = 67.879 g + (1.480 g – 1.209 g) = 68.150 g
		SUM	**69.359**		**SUM**	**69.359**	
26	Drying 3	Product purified with methanol 2	1.209	-	Dried product 3	0.287	-
					Contaminated solvent 4	0.922	$m_{Contaminated\ solvent\ 4}$ = 1.209 g – 0.287 g = 0.922 g
		SUM	**1.209**		**SUM**	**1.209**	
27	Cooling 6	Dried product 3	0.287	-	Final product $SrTiO_3$-0.1/MIL-125-NH_2	0.287	-
		SUM	**0.287**		**SUM**	**0.287**	

Energy balance

PROCESS UNIT	INPUT Calculations/assumptions	Enthalpy (kJ)	OUTPUT Calculations/assumptions	Enthalpy (kJ)
Mixing 1	$\Delta H_{reactants} = \Delta H_{H_2O} + \Delta H_{SrCl_2 \times 6H_2O} + \Delta H_{TiO_2} = (-792.321\ kJ) + (-4.973\ kJ) + (-5.668\ kJ) = -802.962\ kJ$	−802.962	ΔH of the dissolution process of $SrCl_2 \cdot 6H_2O$ in water $(-0.347\ kJ)$	−0.347
Mixing 3	ΔH of Mixing 1 process $(-0.347\ kJ)$ + ΔH of the NaOH $(-21.722\ kJ)$ = −22.069 kJ	−22.069	ΔH of the exothermic process $(1.992\ kJ)$ + ΔH ofthe dissolution process of NaOH in water $(-2.264\ kJ) = -0.272\ kJ$	−0.272
Hydrothermal reaction	ΔH of Mixing 3 process $(-0.272\ kJ)$	−0.272	ΔH of the hydrothermal reaction with change of temperature from 25°C to 180°C $(-0.785\ kJ)$ + energy losses $(7176.686\ kJ)$ = $7175.901\ kJ$	7175.901
Cooling 1	ΔH of the hydrothermal reaction with change of temperature from 25°C to 180°C $(-0.785\ kJ)$	−0.785	ΔH associated with temperature change from 180°C to 25°C $(-34.251\ kJ)$	−34.251
Drying 1	$\Delta H_{reactants} = \Delta H_{SrTiO_3} + \Delta H_{EtOH} + \Delta H_{water} = (-10.531\ kJ) + (-5.358\ kJ) + (-4.800\ kJ) = -20.689\ kJ$	−20.689	ΔH associated with solvents vaporization in 60°C $(1.529\ kJ)$ + energy losses $(3\,241.080\ kJ) = 3242.609\ kJ$	3242.609
Cooling 2	ΔH of Drying 1 process $(1.529\ kJ)$	1.529	ΔH associated with temperature change from 60°C to 25°C $(-0.221\ kJ)$	−0.221
Dissolving	$\Delta H_{reactants} = \Delta H_{DMF} + \Delta H_{MeOH} + \Delta H_{acetic\ acid} + \Delta H_{2-aminoterephthalic\ acid} = (-55.448\ kJ) + (-11.682\ kJ) + (-16.440\ kJ) + (-2.449\ kJ) = -86.019\ kJ$	−86.019	ΔH for the dissolution process of 2-aminoterephthalic acid in DMF $(-0.399\ kJ)$	−0.399
Mixing 6	ΔH of the dissolution process of 2-aminoterephthalic acid in DMF $(-0.399\ kJ)$ + ΔH of the titanium(IV) isopropoxide $(-3.337 kJ)$ + ΔH of the strontium titanate (− 0.165 kJ) = $-3.928\ kJ$	−3.928	ΔH for the dissolution process of titanium(IV) isopropoxide in DMF $(38.058\ kJ)$	38.058
Solvothermal reaction	ΔH of the dissolution process of titanium(IV) isopropoxide in DMF $(38.058\ kJ)$	38.058	ΔH of the solvothermal reaction with change of temperature from 25°C to 150°C $(2.557 kJ)$ + energy losses $(23\,150.621\ kJ) = 23\,153.178\ kJ$	23 153.178
Cooling 3	ΔH of the solvothermal reaction with change of temperature from 25°C to 150°C $(2.557 kJ)$	2.557	ΔH associated with temperature change from 60°C to 25°C $(-5.353\ kJ)$	−5.353
Drying 2	$\Delta H_{reactants} = \Delta H_{SrTiO_3-0.1/MIL-125-NH_2} + \Delta H_{MeOH} = (-0.501\ kJ) + (-7.629\ kJ) = -8.13\ kJ$	−8.13	ΔH associated with methanol vaporization in 60°C $(1.139\ kJ)$ + energy losses $(3\,241.080\ kJ) = 3242.219\ kJ$	3242.219
Cooling 4	ΔH associated with methanol vaporization in 60°C $(1.139\ kJ)$	1.139	ΔH associated with temperature change from 60°C to 25°C $(-0.012\ kJ$	−0.012
Purifying	$\Delta H_{reactants} = \Delta H_{SrTiO_3-0.1/MIL-125-NH_2} + \Delta H_{DMF} = (-0.499\ kJ) + (-119.739\ kJ) = -120.238\ kJ$	−120.238	ΔH associated with temperature change from 25°C to 150°C $(-9.444\ kJ)$ + energy losses $(51\,006.375\ kJ) = 50996.931\ kJ$	50996.931
Cooling 5	ΔH associated with purifying process $(-9.444\ kJ)$	−9.444	ΔH associated with temperature change from 60°C to 25°C $(-9.425\ kJ)$	−9.425
Drying 3	$\Delta H_{reactants} = \Delta H_{SrTiO_3-0.1/MIL-125-NH_2} + \Delta H_{MeOH} = (-0.452\ kJ) + (-6.914\ kJ) = -7.366\ kJ$	−7.366	ΔH associated with methanol vaporization in 60°C $(1.032\ kJ)$ + energy losses $(3\,241.080\ kJ) = 3242.112\ kJ$	3242.112
Cooling 6	ΔH associated with methanol vaporization in 60°C $(1.032\ kJ)$	1.032	ΔH associated with temperature change from 60°C to 25°C $(-0.010\ kJ)$	−0.010

Costs of synthesis

Cost of reagents (current as of 13/03/2024)

No.	Reagent	Producer	Mass/volume	Gross price (PLN)
1	Titanium(IV) oxide, Aeroxide® (P25)	Acros Organics	1 kg	1173.53
2	Strontium chloride hexahydrate	Thermo Scientific	100 g	136.83
3	Sodium hydroxide (NaOH)	STANLAB	1 kg	20
4	Ethyl alcohol, 96%	POCH	1 L	147.48
5	N,n-dimethylformamide (DMF)	POCH	1 L	34.44
6	Acetic acid, 99.5-99.9%	POCH	1 L	25.34
7	Methanol	STANLAB	1 L	14.76
8	2-aminoterephthalic acid, 99%	Thermo Scientific (Acros)	100 g	1684.12

$SrTiO_3$ (1.11 g of product from 1 synthesis)

No.	Reagent	Amount used	Gross price (PLN)
1	Titanium(IV) oxide, Aeroxide® (P25)	0.5 g	0.59
2	Strontium chloride hexahydrate	1.67 g	2.29
3	Sodium hydroxide (NaOH)	2 g	0.04
4	Ethyl alcohol, 96%	30 ml	4.42
			In total: 7.34 PLN 6.61 PLN **per g of product** 6 612.61 PLN **per kg of product**

$SrTiO_3$_large lab scale (12.46 g of product from 1 synthesis)

No.	Reagent	Amount used	Gross price (PLN)
1	Titanium(IV) oxide, Aeroxide® (P25)	5.5 g	6.49
2	Strontium chloride hexahydrate	18.37 g	25.19
3	Sodium hydroxide (NaOH)	22 g	0.44
4	Ethyl alcohol, 96%	90 ml	13.27
			In total: 45.39 PLN 3.64 PLN **per g of product** 3 642.86 PLN **per kg of product**

$SrTiO_3$-0.1/MIL-125-NH_2 (287 mg of product from 1 synthesis)

No.	Reagent	Amount used	Gross price (PLN)
1	$SrTiO_3$ (synthesized in I step)	25 mg	0.09
2	DMF	238 ml	8.20
3	Acetic acid	2 ml	0.05
4	Methanol	182 ml	2.69
5	2-aminoterephthalic acid	0.543 g	9.14
6	Titanium(IV) isopropoxide	0.6 ml	0.53
			In total: 20.7 PLN 72.13 PLN **per g of product** 72 125.44 PLN **per kg of product**

$SrTiO_3$/MIL-125-NH_2_large lab scale_3 (11.463 g of product from 1 synthesis)

No.	Reagent	Amount used	Gross price (PLN)
1	$SrTiO_3$ (synthesized in I step)	600 mg	3.97
2	DMF	2.132 L	73.43
3	Acetic acid	48 ml	1.22
4	Methanol	1.248 L	18.42
5	2-aminoterephthalic acid	13.032 g	219.36
6	Titanium(IV) isopropoxide	14.4 ml	12.72
			In total: 329.12PLN 28.71 PLN **per g of product** 28 711.51 PLN **per kg of product**

$SrTiO_3$/MIL-125-NH_2_pilot scale (177.335 g of product from 1 synthesis)

No.	Reagent	Amount used	Gross price (PLN)
1	$SrTiO_3$ (synthesized in I step)	6 g	39.66
2	DMF	12.32 L	424.37
3	Acetic acid	480 ml	12.2
4	Methanol	6.48 L	95.64
5	2-aminoterephthalic acid	130.32 g	2193.6
6	Titanium(IV) isopropoxide	144 ml	127.2
			In total: 2892.67 PLN 16.31 PLN **per g of product** 16 311.90 PLN **per kg of product**

„Pioneering hybrid materials for CO_2 photoconversion", no NOR/SGS/HotHybrids/0130/2020-00. Project financed by the Financial Mechanism of the European Economic Area (EEA) and the Norwegian Financial Mechanism 2014-2021.

Conclusions

WP1: Development of single and double perovskite synthesis methods

Efforts to introduce double perovskites into MOF synthesis demonstrated their instability, as they degraded in the solvents required for MOF formation and under elevated temperatures. Ultimately, several single perovskites were selected for further investigation, including $CsPbX_3$ (X = Br, I), $Cs_3Bi_2X_9$ (X = I, Br, Cl), and $SrTiO_3$.

WP2: Synthesis of MOFs and their composites suitable for heterogeneous photocatalysis

The goal was to synthesize MOFs that are both theoretically attractive for photocatalytic applications and stable in aqueous solutions for hybrid material development. While various combinations were explored (e.g., $CsPbX_3$@UiO-66, $CsPbX_3$@ZIF-67, $CsPbB_3/SiO_2$@In-MIL-68, Cs_2AgBiBr@UiO-66-NH_2, $CsAgBiBr_6$@ZIF-68), only a few showed significant photocatalytic activity. These included: (i) $CsPbX_3$@UiO-66-Y (X = Br, I; Y = H, NH_2, Br), (ii) $SrTiO_3$@NH_2-MIL-125(Ti), (iii) TiO_2-X@Cs_3BiX_9 (X = Cl, Br, I), (iv) $CuGaS_2$@NH_2-MIL-125(Ti), and (v) Cu-NH_2-MIL-125(Ti).

WP3: Photocatalytic activity analysis

The photocatalytic performance of the hybrids was assessed in H_2 generation and CO_2 photoconversion reactions. All hybrid systems exhibited activity in H_2 generation, while only Cu-NH_2-MIL-125(Ti) demonstrated activity in CO_2 photoconversion.

WP4: Scaling up $SrTiO_3$@NH_2-MIL-125(Ti) hybrid synthesis

A scalable synthesis method for $SrTiO_3$@NH_2-MIL-125(Ti) was developed using a 10-liter batch reactor, yielding over 170 grams per batch. A detailed process flow diagram was created, accompanied by mass and energy balances and an economic analysis.

„Pioneering hybrid materials for CO_2 photoconversion", no NOR/SGS/HotHybrids/0130/2020-00. Project financed by the Financial Mechanism of the European Economic Area (EEA) and the Norwegian Financial Mechanism 2014-2021.